Lattice kinetics of diffusion-limited coalescence and annihilation with sources

Lattice kinetics of diffusion-limited coalescence and annihilation with sources

E Abad[1], T Masser[2] and D ben-Avraham[2]

[1] Centre for Nonlinear Phenomena and Complex Systems, Université Libre de Bruxelles,
Campus Plaine CP 231, B-1050 Bruxelles, Belgium
[2] Physics Department and Clarkson Institute for Statistical Physics, Clarkson University,
Potsdam, NY 13699-5820, USA

E-mail: eabad@ulb.ac.be and benavraham@clarkson.edu

Abstract
We study the one-dimensional kinetics of diffusion-limited coalescence and
annihilation with back reactions and different kinds of particle input. By
considering the changes in occupation and parity of a given interval, we derive
sets of hierarchical equations from which exact expressions for the lattice
coverage and the particle concentration can be obtained. We compare the mean-
field approximation and the continuum approximation to the exact solutions and
we discuss their regime of validity.

PACS numbers: 02.50.Ey, 05.50.+q, 05.70.Ln, 82.40.-g

1. Introduction

A standard way of studying the kinetics of reaction-diffusion systems involves derivation of an
infinite set of moment equations for the state probability. The solution of such equations
usually poses great mathematical difficulties; however, the simple topology of the one-
dimensional (1D) lattice frequently allows derivation of exact solutions [1–6]. These results
may be used to test the validity of various approximations. Neglecting spatial fluctuations
in concentration and occupation number space leads to classical macroscopic rate equations.
This type of approximation, which implicitly assumes that each particle interacts with the
system as a whole through a *mean field* (MF), should improve as the number of interacting
neighbours grows, i.e. with increasing dimensionality of the lattice. Although this approach
may seem too rough for one-dimensional systems, it works well for early time evolution and
in other situations where the distribution of particles is nearly free of correlations.

Exactly solvable reaction-diffusion models consist largely of single species reactions in one dimension, e.g. variations of the coalescence process, $A + A \rightarrow A + S$ [7–12] and the annihilation process $A + A \rightarrow S + S$ [10, 11, 13–21], where A and S denote empty and occupied sites, respectively. These simple reactions display a wide range of behaviour characteristic of non-equilibrium kinetics, such as self-organization, pattern formation and kinetic phase transitions. Interval methods have provided many exact solutions for one-dimensional coalescence and annihilation models. The method of empty intervals, applicable to coalescence models, requires solution of an infinite hierarchy of differential difference equations for the probabilities E_n of finding n consecutive lattice sites simultaneously empty [7–9, 12, 22–24]. For annihilation models, the method of parity intervals similarly requires determination of G_n, the probability of n consecutive lattice sites containing an even number of particles [25–27].

The infinite hierarchy of equations for the interval probabilities can be used as a starting point for the derivation of MF and continuum approximations. Most results obtained from interval methods rely on a continuum approximation of the spatially discrete equations; the resulting PDEs allow for straightforward solution. However, the pertinent set of differential difference equations for the interval probabilities admits analytical solutions [28], providing exact results which may differ from the continuum limit. In general, we expect that this discrepancy becomes important for high concentrations and short timescales (compared to the typical reaction time), since on-lattice local concentration perturbations travel at finite speed, in contrast to propagation in a spatial continuum.

In this work, we use the interval methods described above to study the on-lattice kinetics of coagulation and annihilation reactions including particle creation steps. Explicit expressions for the lattice coverage and the concentration are derived and compared to those yielded by the MF and the continuum approximation. The behaviour of coalescence and annihilation changes qualitatively if the reaction schemes incorporate particle sources in the form of input (external source) or back reactions (internal source). In the absence of sources, the concentration displays an anomalous $t^{-1/2}$-decay to an empty, steady state [18, 19]. Particle sources give rise to steady states with nonzero concentration and change the transient behaviour [9, 15]. In most cases, the concentration may be thought of as an order parameter in a 'phase transition' between the empty and the active steady state, which is controlled by the effective rate of particle creation, h. In analogy to the theory of critical phenomena, one can regard $h = 0$ as a transition point and characterize the steady state and the relaxation time of the system near the critical point through a set of static and dynamical exponents [29]. We shall see that our method allows the characterization of the system not only near the phase transition, but also far beyond criticality.

This work is organized as follows. In section 2, we define the general form of the coalescence model and solve for the cases in which the back reaction or a homogeneous particle input is present. The validity of MF-like rate equations and the continuum approximation is analysed vis-a-vis the exact solution. In section 3, we do the same for the annihilation model with different kinds of particle input. Similarities with Glauber-type spin models and the relevance of these models to physical systems are briefly discussed. We also treat an annihilation model with symmetric birth [30], both with immobile and diffusing reactants. We conclude in section 4 with a summary of our results and possible extensions of this work.

2. Coalescence models

All reactions in sections 2 and 3 are defined on an infinite one-dimensional lattice with spacing a. The basic coalescence model involves particles moving randomly and asynchronously to nearest-neighbour sites with hopping rate $2D/a^2$; in an extended model, particles give birth, i.e. a particle at a given site generates offspring at an empty adjacent site at the rate v/a. One

can also include a homogeneous source: particles are injected into the lattice at rate Ra. In all cases, a particle disappears whenever it lands on another. Let $E_n(t)$ be the probability that a randomly chosen segment of n consecutive sites contains no particles. By noting the changes in E_n during a small time interval, Δt, and taking the continuous time limit $\Delta t \to 0$, we derive the Master equation [7]:

$$\frac{dE_n}{dt} = \frac{2D}{a^2}(E_{n+1} - 2E_n + E_{n-1}) + \frac{v}{a}(E_{n+1} - E_n) - RnaE_n. \tag{1}$$

The first term on the right-hand side represents the effect of the net particle flow into and out of an empty interval, whereas the second and third terms describe the effect of the back reaction (cooperative particle birth) and a homogeneous particle input, respectively. By comparing (1) for $n = 1$ to the changes in E_1 during a time interval Δt, one arrives at the boundary condition $E_0(t) = 1$. Also, for non-empty lattices, $E_\infty(t) = 0$. The case $D > 0, v = R = 0$ has already been solved in a previous paper [28]. In that case, the reaction displays universal, anomalously slow $t^{-1/2}$-decay to an empty state, as opposed to the MF t^{-1} asymptotic decay. This result holds both on-lattice and in the continuum limit [28], and is reminiscent of persistent transient fluctuations induced by the dynamic self-ordering of the system [7].

In what follows, we focus on the cases $D > 0, v > 0, R = 0$ (reversible coalescence $A + A \rightleftharpoons A + S$, subsection 2.1) and $D > 0, v = 0, R > 0$ (coalescence with input, subsection 2.2). We use the initial condition

$$E_n(0) = (1 - \rho_0)^n. \tag{2}$$

This corresponds to a random homogeneous distribution of particles characterized by a global coverage ρ_0 and a concentration (the number of particles per unit length) $c_0 = \rho_0/a$. Our primary goal is to compute the time evolution of the global coverage $\rho(t) = 1 - E_1(t)$ and the associated concentration $c(t) = \rho(t)/a$.

2.1. Reversible coalescence

The existence of a kinetic phase transition for this system in the continuum limit is well known [8]. Recently, Lin has shown that the phase transition is not an artefact of the continuum limit, since asymptotically this approximation only gives rise to quantitative corrections [31]. To do so, he solved the corresponding empty interval hierarchy by mapping it into a spin system with Glauber dynamics. However, it is possible to solve the hierarchy more straightforwardly by means of a simple Laplace transform (LT) method, as we show below.

The boundary value problem (BVP) of interest is [8]

$$\frac{dE_n}{d\tau} = E_{n+1} - 2E_n + E_{n-1} + h(E_{n+1} - E_n) \tag{3}$$

where $\tau = 2Dt/a^2$ is a dimensionless time and $h = va/2D$ is the relative feed rate; the boundary conditions read $E_0(\tau) = 1$ and $E_\infty(t) = 0$, and the random homogeneous initial condition is that given by (2). First, we solve for the steady state $E_{n,s}$. Setting $\frac{dE_n}{d\tau} = 0$ on the left-hand side of equation (3), we get

$$(1 + h)E_{n+1,s} - (2 + h)E_{n,s} + E_{n-1,s} = 0. \tag{4}$$

This difference equation has the solution

$$E_{n,s} = (1 + h)^{-n} \tag{5}$$

whence the steady state concentration is obtained:

$$c_s = \frac{\rho_s}{a} = \frac{1 - E_{1,s}}{a} = \frac{v}{2D + va}. \tag{6}$$

It has been shown that this is a true equilibrium steady state characterized by the presence of detailed balance and a maximum of the entropy [8]. The spatial coherence induced by the coalescence reaction is eventually destroyed by the back reaction.

Equation (3) may be solved by standard techniques, for example, by taking the LT with respect to τ, fitting a power ansatz to the resulting difference equation, and finally inverting the LT of the solution. With the boundary data $E_0(t) = 1$ and $E_\infty(t) = 0$, the LT of $E_1(t)$ is given by

$$\hat{E}_1(s) = \left(\frac{1}{s} - \frac{1}{s+\beta}\right)\left(\frac{s+2+h-\sqrt{(s+2+h)^2-4(1+h)}}{2(1+h)}\right) + \frac{(1-\rho_0)}{s+\beta} \tag{7}$$

where $\beta = h\rho_0 - \rho_0^2/(1-\rho_0)$. Using the faltung theorem for the LT [32], this can be inverted to yield

$$E_1(\tau) = \frac{1}{\sqrt{1+h}}\int_0^\tau e^{-(2+h)\tau'} I_1\left(2\sqrt{1+h}\tau'\right)\frac{d\tau'}{\tau'}$$

$$+ e^{-\beta\tau}\left[1 - \rho_0 - \frac{1}{\sqrt{1+h}}\int_0^\tau e^{-(2+h-\beta)\tau'} I_1\left(2\sqrt{1+h}\tau'\right)\frac{d\tau'}{\tau'}\right] \tag{8}$$

where $I_n(\cdot)$ is the nth order modified Bessel function. If the lattice is completely filled initially ($\rho_0 \to 1$), the difference equations for $\hat{E}_n(s)$ are homogeneous and the second term on the right-hand side of (8) vanishes.

Using the $s \to \infty$ expansion of $\hat{E}_1$ facilitates investigation of the short time behaviour:

$$\hat{E}_1(s) = \frac{1-\rho_0}{s} - \frac{\beta(1-\rho_0)}{s^2} + \mathcal{O}(s^{-3}). \tag{9}$$

By virtue of a Tauberian theorem [33, 34], we obtain

$$\rho(\tau) = \rho_0 + \left[h\rho_0(1-\rho_0) - \rho_0^2\right]\tau + \mathcal{O}(\tau^2) \qquad \tau \to 0 \tag{10}$$

for the short-time site occupancy.

In the opposite limit, the expansion of $\hat{E}_1(s)$ about $s = 0$ provides no additional information about the long time solution; only the steady state solution is recovered. Determining the long time asymptotics requires a bit more work. We write $E_1(\tau)$ as

$$E_1(\tau) = 1 - \rho_s - \frac{2}{\gamma}\int_\tau^\infty e^{-\alpha\tau'} I_1(\gamma\tau')\frac{d\tau'}{\tau'}$$

$$+ \left[1 - \rho_0 - U + \frac{2}{\gamma}\int_\tau^\infty e^{-(\alpha-\beta)\tau'} I_1(\gamma\tau')\frac{d\tau'}{\tau'}\right]e^{-\beta\tau} \tag{11}$$

with the notation

$$\alpha = 2 + h \qquad \gamma = 2\sqrt{1+h} \qquad \rho_s = \frac{h}{1+h}$$

$$U = \frac{2}{\gamma}\int_0^\infty e^{-(\alpha-\beta)\tau'} I_1(\gamma\tau')\frac{d\tau'}{\tau'}. \tag{12}$$

All integrals in $E_1(\tau)$ converge, since $\alpha - \beta \geqslant \gamma$. Moreover, U is a known LT:

$$U = \frac{2}{\gamma^2}\left(\alpha - \beta - \sqrt{(\alpha-\beta)^2 - \gamma^2}\right). \tag{13}$$

Based on the value of the initial coverage, ρ_0, there are three cases for U:

$$U = \begin{cases} 1 - \rho_0 & \text{for} \quad \rho_0 > \rho_c \\ \dfrac{1}{\sqrt{h+1}} & \text{for} \quad \rho_0 = \rho_c \\ \dfrac{1}{(h+1)(1-\rho_0)} & \text{for} \quad \rho_0 < \rho_c \end{cases} \tag{14}$$

where $\rho_c \equiv 1 - \sqrt{1 - \rho_s}$ is a critical initial coverage. One has $\rho_c < \rho_s$, and $\rho_c \to \frac{1}{2}\rho_s$ as $h \to 0$.

For long times, the asymptotic form of $I_1(z)$ [35] may be used to approximate the remaining integrals in the expression for $E_1(\tau)$. We then have the following asymptotic formula for the coverage:

$$\rho(\tau) - \rho_s \approx \begin{cases} -\sqrt{\dfrac{2}{\pi\gamma^3}}\dfrac{\beta\tau^{-3/2}e^{-(\alpha-\gamma)\tau}}{(\alpha - \beta - \gamma)(\alpha - \gamma)} & \text{for} \quad \rho_0 > \rho_c \\[3ex] -\sqrt{\dfrac{8}{\pi\gamma^3}}\tau^{-1/2}e^{-(\alpha-\gamma)\tau} & \text{for} \quad \rho_0 = \rho_c \\[3ex] -\left(1 - \rho_0 - \dfrac{1}{(h+1)(1-\rho_0)}\right)e^{-\beta\tau} & \text{for} \quad \rho_0 < \rho_c. \end{cases} \tag{15}$$

Considering then the (dimensionless) relaxation time τ_R, defined as

$$\tau_R^{-1} \equiv -\lim_{\tau\to\infty}\tau^{-1}\ln|\rho(\tau) - \rho_s| \tag{16}$$

we see that the system undergoes a second-order dynamical phase transition, from a slowly relaxing phase—with τ_R dependent on ρ_0—for $\rho_0 < \rho_c$, to a phase with constant τ_R, for $\rho_0 > \rho_c$. It can be readily shown that the first derivative of τ_R at $\rho_0 = \rho_c$ is continuous, while the second derivative displays a finite jump determined by the value of h.

MF and continuum approach. We now examine the simplest type of MF approximation for reversible coalescence. In this approach, the kinetics of ρ may be obtained either by means of simple heuristic arguments or directly from the empty interval hierarchy. Let P_n be the probability of n consecutive sites being simultaneously occupied. Making use of the identities $E_1 = 1 - P_1$ and $E_2 = 1 - 2P_1 + P_2$ in the evolution equation for E_1, we have

$$\frac{dP_1}{d\tau} = -(1+h)P_2 + hP_1. \tag{17}$$

Neglecting spatial correlations amounts to setting $P_2 = P_1^2$ in this equation. Taking into account that P_1 is identical with the mean site occupation ρ, we get

$$\frac{d\rho}{d\tau} = -(1+h)\rho^2 + h\rho. \tag{18}$$

The physically acceptable steady state of this equation is given by

$$\rho_s^{\mathrm{MF}} = \rho_s = \frac{h}{1+h}. \tag{19}$$

The time-dependent solution matching this steady state is

$$\rho^{\mathrm{MF}} = \frac{h}{[(h/\rho_0) - 1 - h]e^{-h\tau} + 1 + h}. \tag{20}$$

For short times, the Taylor expansion of the exponential function yields (10); as expected, the MF approach is a good approximation at early times. In the opposite, long-time limit, an exponential relaxation towards the equilibrium steady state occurs:

$$\rho^{\mathrm{MF}} - \rho_s \propto \rho_s\left[1 - \frac{\rho_s}{\rho_0}\right]e^{-h\tau} \qquad \tau \to \infty. \tag{21}$$

Thus, in the MF approach, τ_R is given by
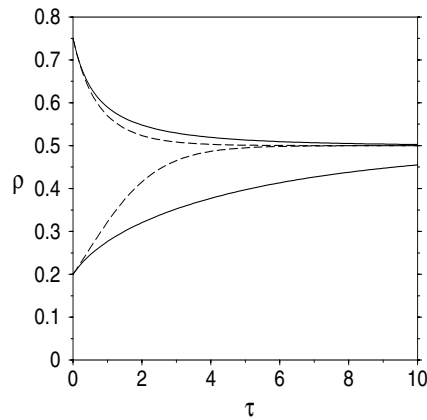
$$\tau_R = h^{-1}. \tag{22}$$

Figure 1. Exact lattice coverage (solid curves) versus MF approximation (dashed curves) of the reversible coalescence for two different initial conditions $\rho_0 = 0.75$ and 0.2 ($h = 1$). Since $0.2 < 0.29 \approx \rho_c$, the exact solution relaxes much slowlier into the equilibrium steady state in the latter case.

This result is universal in the sense that the relaxation time does not 'remember' the initial condition ρ_0, which is only contained in the prefactor $1 - \rho_s/\rho_0$.

If the initial coverage is low enough, the relaxation towards equilibrium is basically given by the time taken to fill large gaps through particle birth from the edge sites [8]. Therefore, τ_R becomes initial-condition dependent in this regime, in contrast to the MF result (cf figure 1). Moreover, τ_R becomes arbitrarily large in the limit $\rho_0 \to 0$. On the other hand, if $\rho_0 > \rho_c$, τ_R is MF-like only for large h. Note, however, that the relaxation is not purely exponential, since additional powers of τ appear in the asymptotic form of the exact solution of equation (15).

The exact results can also be compared with the continuum approximation, where one lets the lattice constant a shrink to zero [31]. To this end, we rewrite (10) in terms of concentration, using $c_s = (1/a)\, h/(1+h)$ and $2D/v^2$ as the units of concentration and time, respectively:

$$c = c_0 + \frac{c_0(1-c_0)}{h}t + \mathcal{O}(t^2) \tag{23}$$

where c and t are dimensionless now. On the other hand, rescaling c and t as above and taking the limit $h \to 0$ for fixed R and D in the long time form of the solution, equation (15), yields

$$c = \begin{cases} 1 + 2\pi^{-1/2}[1 - (1 - 2c_0)^{-2}]t^{-3/2}e^{-t/4} & \text{for} \quad c_0 > 1/2 \\ 1 - \pi^{-1/2}t^{-1/2}e^{-t/4} & \text{for} \quad c_0 = 1/2 \\ 1 - (1 - 2c_0)e^{-c_0(1-c_0)t} & \text{for} \quad 0 < c_0 < 1/2. \end{cases} \tag{24}$$

An alternative way to perform the continuum approximation consists of replacing the set of difference equations (3) by the PDE

$$\frac{\partial E(x,t)}{\partial t} = 2D\frac{\partial^2 E}{\partial x^2} + v\frac{\partial E}{\partial x} \tag{25}$$

for a spatially continuous function $E(x,t)$, the boundary conditions now being $E(0,t) = 1$ and $E(\infty, t) = 0$. This equation can be solved for $E(x,t)$ with a suitable exponential ansatz [8]; the global concentration $c(t)$ is then obtained by deriving with respect to space:

$$c(t) = -\left.\frac{\partial E(x,t)}{\partial x}\right|_{x=0}. \tag{26}$$

Eventually, one can rescale c and t in dimensionless units as done above to obtain

$$c(t) = 1 - \tfrac{1}{2}\mathrm{erfc}\left(\tfrac{1}{2}\sqrt{t}\right) + |\tfrac{1}{2} - c_0|e^{-c_0(1-c_0)t}\left[\mathrm{erfc}\left(|\tfrac{1}{2} - c_0|\sqrt{t}\right) - 2\Theta(\tfrac{1}{2} - c_0)\right] \tag{27}$$

where $\Theta(\cdot)$ is the Heaviside step function. As expected, the long time development of this expression is identical to (24). In contrast, for short times one has

$$c(t) = c_0 + \left(\frac{1}{2\sqrt{\pi}} - 2\frac{(1/2 - c_0)^2}{\sqrt{\pi}}\right)\sqrt{t} + (1/2 - c_0)c_0(1 - c_0)t + \mathcal{O}(t^{3/2}). \tag{28}$$

Thus, for early times there is a qualitative discrepancy with respect to the on-lattice case, even as $c_0 \to 0$. The evolution is initially faster in a continuum, due to the infinite speed of propagation of local perturbations.

2.2. Coalescence with input

As a second example, we consider the effect of a homogeneous external input $S \to A$, at rate Ra, on the simple coalescence reaction. This model is described by the set of equations [7]:

$$\frac{dE_n}{d\tau} = E_{n-1} - (2 + hn)E_n + E_{n+1} \tag{29}$$

with the boundary conditions $E_0 = 1$ and $E_\infty = 0$, where we used the dimensionless time $\tau = 2Dt/a^2$ and relative feed rate $h = Ra^3/2D$.

We now compute the exact steady state solution by setting the left-hand side of (29) equal to zero. The resulting set of difference equations can be compared to recursion relations satisfied by the Bessel functions [35]:

$$J_{\nu-1}(z) - \frac{2\nu}{z}J_\nu(z) + J_{\nu+1}(z) = 0. \tag{30}$$

The boundary condition at the origin determines the appropriate normalization factor for the steady state solution, $E_{n,s}$. The steady state coverage is then given by

$$\rho_s = 1 - \frac{J_{2h^{-1}+1}(2h^{-1})}{J_{2h^{-1}}(2h^{-1})}. \tag{31}$$

For $h \ll 1$ we can use the Taylor expansion of $J_{x+\Delta x}(x)$ around x to obtain

$$\rho_s \approx -\frac{1}{J_{2h^{-1}}(2h^{-1})}\frac{d}{dx}J_x(2h^{-1})\bigg|_{x=2h^{-1}}. \tag{32}$$

We compute the derivative of the Bessel function by using the asymptotic form [35]

$$J_\nu(\nu + z\nu^{1/3}) = 2^{1/3}\nu^{-1/3}\mathrm{Ai}(-2^{1/3}z) + \mathrm{O}(\nu^{-1}) \qquad \nu \to \infty \tag{33}$$

(where $\mathrm{Ai}(\cdot)$ denotes the Airy function) and obtain an explicit expression for the small-h limit of the stationary coverage:

$$\rho_s = \frac{|\mathrm{Ai}'(0)|}{\mathrm{Ai}(0)}h^{1/3} \qquad h \to 0. \tag{34}$$

In the opposite limit, $h \to \infty$, we have the following result:

$$\rho_s = 1 - h^{-1} \qquad h \to \infty. \tag{35}$$

Let us now examine the early time kinetics of our model. In general, it is difficult to obtain a closed solution of the hierarchy (29) because of the nonconstant coefficient of E_n on the right-hand side. Under the simplifying assumption of an initially full lattice, we take the LT of (29) and get

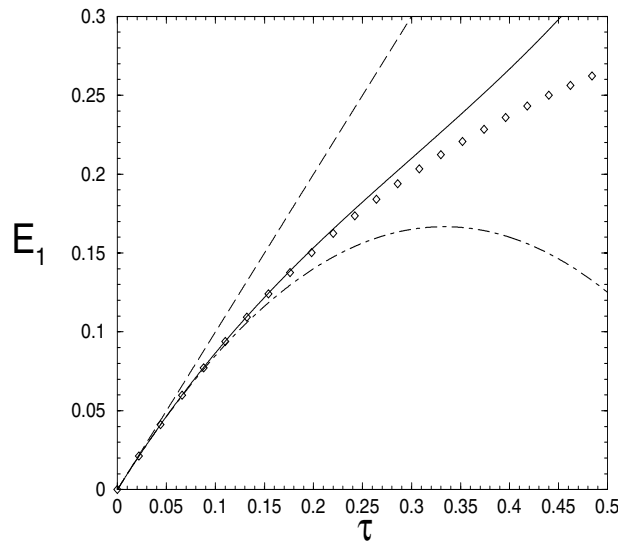$$\hat{E}_{n-1} - (2 + s + hn)\hat{E}_n + \hat{E}_{n+1} = 0 \tag{36}$$

Figure 2. Comparison of the approximations of E_1 obtained by truncating the series expansion (40) to first order (dashed), second order (dashed–dotted) and third order (solid) with the exact solution (diamonds). The relative feed rate is $h = 1$.

with $\hat{E}_0 = 1/s$ and $\hat{E}_\infty = 0$. Exploiting again the analogy of equation (36) with the recursion relations for the Bessel functions and using the boundary conditions leads to

$$\hat{E}_n = \frac{1}{s} \frac{J_{(2+s)h^{-1}+n}(2h^{-1})}{J_{(2+s)h^{-1}}(2h^{-1})}. \tag{37}$$

For $s \to 0$, one recovers (31) by making use of the theorem $\lim_{s \to 0} s\, \hat{E}_n = E_n(\infty)$. Since the conjugate time variable s appears in the index of the Bessel functions, the exact inversion of (37) is quite involved. Instead, it is better to work with an asymptotic formula. For $n = 1$, we can express $\hat{E}_1$ as a continued fraction [35]:

$$\hat{E}_1(s) = \left(\frac{1}{s}\right) \cfrac{1}{s+2+h - \cfrac{1}{s+2+2h - \cfrac{1}{s+2+3h - \cdots}}}. \tag{38}$$

We can now expand the right-hand side in powers of s^{-1} by using the Stieltjes method for J-fractions [36] and find

$$\hat{E}_1(s) = \frac{1}{s^2} - \frac{2+h}{s^3} + \frac{(2+h)^2 + 1}{s^4} + \mathcal{O}\left(\frac{1}{s^5}\right). \tag{39}$$

Inverting this expression term by term, we obtain the early time behaviour of the empty-site coverage (cf figure 2):

$$\rho(\tau) = 1 - \tau + \left(1 + \frac{h}{2}\right)\tau^2 - \frac{(2+h)^2 + 1}{6}\tau^3 + \mathcal{O}(\tau^4) \qquad \tau \to 0. \tag{40}$$

The continued fraction representation of the LT is not suitable for obtaining the long-time asymptotics. Instead, we make an exponential ansatz directly in equation (29):

$$E_n(\tau) = E_{n,s} + a_n\, e^{-2\lambda\tau}. \tag{41}$$

The calculation of τ_R follows the guidelines laid by Rácz for annihilation with input (see [15] and subsection 3.1). Substituting equation (41) in the set of differential-difference equation (29), one finds that the coefficients a_n obey the same set of equations as E_n, except that $1 + nh/2$ is now replaced by $1 - \lambda + nh/2$. Using the boundary condition at $n = 0$, we find the equation for the possible values of λ:

$$J_{(1-\lambda)2h^{-1}}(2h^{-1}) = 0. \tag{42}$$

All the solutions $\lambda_i(h)$ are positive, since the zeros j_i^ν of the Bessel functions satisfy the inequality $\nu < j_i^\nu$ [35], meaning that all homogeneous perturbations around the steady state decay exponentially with time. The small-h limit is carried out using the asymptotic form (33). Setting $\nu = 2(1 - \lambda)h^{-1}$ and $z = \nu^{2/3}/(1 - \lambda)$ yields

$$\mathrm{Ai}(-2\,h^{-2/3}\lambda/(1 - \lambda)^{1/3}) = 0. \tag{43}$$

From this, a cubic equation for λ can be extracted,

$$\lambda_j^3 + p\lambda_j - p = 0 \qquad p = \frac{|a_j|^3}{8}h^2 \tag{44}$$

where a_j are the zeros of the Airy function. Since the discriminant $\Delta = (p/3)^3 + (p/2)^2$ is positive, this equation has two unphysical complex solutions and one real solution, the latter of which is given by Cardan's formula:

$$\lambda_j = u + v \qquad u = (p/2 + \sqrt{\Delta})^{1/3} \qquad v = -\frac{3p}{u}. \tag{45}$$

Expanding this expression for small h, we find the smallest eigenvalue

$$\lambda_1 = \frac{|a_1|}{2}\,h^{2/3} \qquad h \to 0 \tag{46}$$

from which we obtain

$$\tau_R^{-1} = 2\,\lambda_1 = |a_1|\,h^{2/3} + \mathcal{O}(h^{4/3}). \tag{47}$$

The corresponding MF equation for $\rho(\tau)$ may be obtained following the procedure of the preceding section. We find

$$\frac{\mathrm{d}\rho}{\mathrm{d}\tau} = -\rho^2 + h\,(1 - \rho). \tag{48}$$

Integrating and using the initial condition, we obtain

$$\rho^{\mathrm{MF}} = \frac{\rho_+ - \sigma\,\rho_-\,\mathrm{e}^{-\eta\tau}}{1 - \sigma\,\mathrm{e}^{-\eta\tau}} \tag{49}$$

where $\eta = \sqrt{h^2 + 4h}$, $\rho_\pm = (-h \pm \eta)/2$ and $\sigma = (\rho_0 - \rho_+)/(\rho_0 - \rho_-)$. The predicted long time coverage is $\rho^{\mathrm{MF}}(\infty) \equiv \rho_s^{\mathrm{MF}} = \rho_+$. For small h, the steady state coverage is

$$\rho_s^{\mathrm{MF}} = h^{1/2} + \mathcal{O}(h) \tag{50}$$

whereas for large h we get

$$\rho_s^{\mathrm{MF}} = 1 - h^{-1} + \mathcal{O}(h^{-2}). \tag{51}$$

We now examine the transient behaviour of the MF approximation. Taking $\rho_0 = 1$, i.e. an initially full lattice, the early time kinetics is

$$\rho^{\mathrm{MF}} = 1 - \tau + \left(1 + \frac{h}{2}\right)\tau^2 + \mathcal{O}(\tau^3) \qquad \tau \to 0 \tag{52}$$

while the long-time behaviour for an arbitrary ρ_0 is found to be

$$\rho^{\mathrm{MF}} \approx \rho_+ + \sigma\,\eta\,\mathrm{e}^{-\eta\tau} \qquad \tau \to \infty. \tag{53}$$
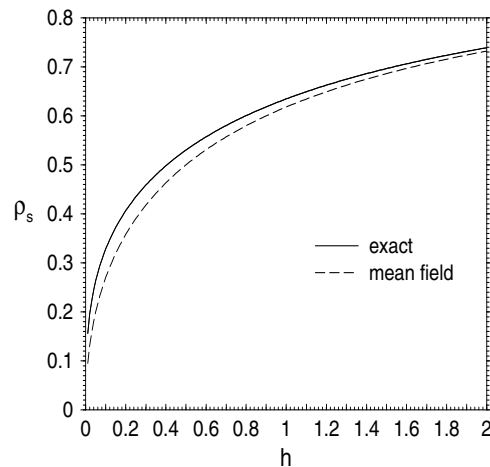
Figure 3. Comparison of the steady state coverage as a function of the relative feed rate h computed from the exact solution and the MF approach.

Thus, the inverse relaxation time is

$$\tau_R^{-1} \approx 2 h^{1/2} \qquad h \to 0 \tag{54}$$

and

$$\tau_R^{-1} \approx h \qquad h \to \infty. \tag{55}$$

It is worth making a few comments on the MF approximation. For $h = 0$ (no input), the MF equation predicts in both cases a t^{-1} decay towards an empty steady state. However, if h is finite, the decay becomes exponential with a relaxation time that diverges as $h^{-1/2}$ for small h. This observation suggests that $h = 0$ can be viewed as a transition point, and one can try to account for spatial fluctuations by some kind of phenomenological scaling assumption inspired by the theory of critical phenomena [29]. On the other hand, the limit $h \to 0$ for fixed R and D considered here automatically realizes the continuum approximation $a \to 0$. As expected, ρ_s approaches zero in this limit, but the exact solution is larger than MF ($\rho_s \propto h^{1/3}$ versus $\rho_s^{MF} \propto h^{1/2}$). Moreover, the exact solution remains larger than the MF approximation over the whole h range (figure 3). This is not surprising, since the coalescence step responsible for particle removal requires that interacting particles occupy neighbouring sites, while in the MF approximation the effective range of the interaction is arbitrarily large. On the other hand, as h becomes large, the exact steady state approaches the MF curve[3] given by equation (51) (cf figure 3). This result is quite natural, since the input mechanism involves no spatial correlations. For sufficiently small h, the system relaxes more slowly into the steady state than the MF prediction ($\tau_R^{-1} \propto h^{2/3}$ as opposed to $\tau_R^{-1} \propto h^{1/2}$ in the MF case). In the large-h limit, an expansion of the real root of (44) shows that $\tau_R^{-1} \propto h$, as expected from the MF approximation. The results (34) for the stationary coverage and (47) for the relaxation time in the small input limit are in full agreement with the corresponding continuum approximation [9]. However, one expects a discrepancy for early times, as observed for reversible coalescence.

---

[3] This can also be checked analytically by using the ascending series expansion of the Bessel function $J_\nu(x) = \sum_{k=0}^{\infty} \frac{(-x^2/4)^{k+\nu}}{k!\,\Gamma(\nu+k+1)}$.

3. Annihilation models

The basic model consists of diffusing point particles that annihilate upon contact. The particles hop with probability $2D/a^2$ to nearest-neighbour sites; the only difference from simple coalescence is that here *both* particles vanish instantaneously whenever they attempt to occupy the same site. This reaction scheme conserves the parity of the total number of particles. Parity changes in a given interval may only arise by particle migration into or out of the interval. The evolution of $G_n(t)$, the probability that n consecutive sites contain an even number of particles, provides detailed information about the annihilation process $A + A \to S + S$. Following similar arguments as those for coalescence, one arrives at [25]

$$\frac{dG_n}{d\tau} = G_{n-1} - 2G_n + G_{n+1}. \tag{56}$$

The boundary conditions are $G_0 = 1$ and $0 \leqslant G_n \leqslant 1$. Note the similarity between the equations for G_n (for annihilation) and E_n (for coalescence). Indeed, it has been shown that the basic coalescence and annihilation models lie in the same universality class [37]; in the framework of our interval method, one can show that the only difference between coalescence, annihilation and the zero-temperature q-state Potts model stems from the specific form of the various initial conditions [25]. In the present case, if the lattice has a random distribution of particles with global coverage ρ_0, a simple combinatorial argument yields

$$G_n(0) = \tfrac{1}{2} + \tfrac{1}{2}(1 - 2\rho_0)^n. \tag{57}$$

As predicted by early works of Torney and McConnell [13], and Lushnikov [14], the exact solution of (56) (on- and off-lattice) shows an anomalous, asymptotic $\tau^{-1/2}$ decay of the lattice coverage $\rho = 1 - G_1$ to the empty steady state.

The annihilation model may be extended by including input or birth processes. In the following, we present exact results concerning some of these possibilities.

3.1. Single-particle input

At each time step a particle is injected at a randomly chosen site at rate Ra. The site becomes occupied if it is initially empty and becomes empty otherwise. This is equivalent to adding the toggle reactions $S \to A$ and $A \to S$ to the original annihilation scheme. The relevant set of equations for the probabilities G_n now reads

$$\frac{dG_n}{d\tau} = G_{n-1} - 2G_n + G_{n+1} + n\,h(1 - 2G_n) \tag{58}$$

with the same boundary conditions as above. Here, the last term represents parity changes due to particle input, and $\tau = 2Dt/a^2$ and $h = Ra^3/2D$.

The model turns out to be closely related to the case of coalescence with input studied above. Indeed, equation (58) may be solved with similar techniques to those used in subsection 2.2. The stationary coverage can be expressed in terms of Bessel functions, and for low h it is smaller than (34) by a factor of $2^{-2/3}$. The relaxation time turns out to be smaller than that for coalescence by a factor of $2^{-2/3}$ [9].

These results are in full agreement with previous calculations by Rácz, who provided an exact solution by mapping the above dynamics into a kinetic Ising model [15]. In Rácz's model, the time evolution of an infinite one-dimensional array $\{\sigma\} \equiv \{\ldots, \sigma_i, \sigma_{i+1}, \ldots\}$ of stochastic pseudo-spin variables $\sigma_i(t) = \pm 1$ is considered; particles are identified with domain walls between regions containing up or down spins only, i.e. the bond variables $n_i \equiv (1 - \sigma_i\sigma_{i+1})/2$ are seen as particle occupation numbers. For random homogeneous initial conditions, translational invariance holds, and the mean (global) particle coverage is

given by $\rho(t) = (1 - \langle \sigma_i \sigma_{i+1} \rangle)/2$. The state probability $P(\{\sigma\}, t)$ satisfies the Glauber master equation

$$\frac{dP(\{\sigma\}, t)}{dt} = \sum_{i=-\infty}^{\infty} \sum_{\alpha=1}^{2} [w_i^{(\alpha)}(\{\sigma\}_i^\alpha) P(\{\sigma\}_i^\alpha, t) - w_i^{(\alpha)}(\{\sigma\}) P(\{\sigma\}, t)] \quad (59)$$

where the state $\{\sigma\}_i^1$ is obtained from $\{\sigma\}$ by flipping the ith spin, and $\{\sigma\}_i^2$ differs from $\{\sigma\}$ by the simultaneous flipping of all spins σ_j with $j \leqslant i$. The flipping rates are given by

$$w_i^{(1)}(\{\sigma\}) = \frac{\Gamma}{2} \left[1 - \frac{\delta}{2} \sigma_i(\sigma_{i+1} + \sigma_{i-1}) \right] \qquad w_i^{(2)}(\{\sigma\}) = \Gamma h. \quad (60)$$

Setting $\delta = 1$ and $\Gamma = 2D/a^2$ corresponds exactly to the dynamics of our model with a relative feed rate h.

It has also been suggested that annihilation with single-particle input may be relevant to the kinetics of a certain class of processes involving cluster–cluster aggregation in the presence of sources and sinks. For example, in aerosol formation aggregation centres can be generated by photo-oxidation, and large clusters may disappear as a result of sedimentation [38]. According to Rácz, it should be expected that such models be in the same universality class as annihilation with input [15].

3.2. Input of adjacent pairs

Pairs of particles are injected simultaneously at adjacent sites at rate R per site per unit time. Thus, the steps $SS \rightarrow AA$, $AS \rightarrow SA$, $SA \rightarrow AS$ and $AA \rightarrow SS$ take place at equal rates (but generically different from the hopping rate for diffusion and annihilation events). The kinetics is described by the equations

$$\frac{dG_n}{d\tau} = G_{n-1} - 2G_n + G_{n+1} + 2h(1 - 2G_n) \quad (61)$$

with $\tau = 2Dt/a^2$ and $h = Ra^2/(2D)$. The boundary conditions remain the same as before.

Again, we begin our study of this model with the steady state solution

$$G_{n,s} = \tfrac{1}{2} + \tfrac{1}{2} \left[1 + 2h - \sqrt{(1+2h)^2 - 1} \right]^n. \quad (62)$$

This implies a steady state coverage of

$$\rho_s = \sqrt{h^2 + h} - h. \quad (63)$$

For fast input rates (large h), we have

$$\rho_s \approx \frac{1}{2} - \frac{1}{8h} \qquad h \rightarrow \infty \quad (64)$$

while for small h,

$$\rho_s \approx h^{-1/2} \qquad h \rightarrow 0. \quad (65)$$

We now derive the exact time dependence of the concentration for a random homogeneous initial distribution. Applying the LT to both sides of (61) and using the initial condition (57) yields a set of inhomogeneous difference equations. However, the inhomogeneity does not depend on n and can be easily shifted away. After using the boundary conditions, we obtain

$$\hat{G}_n = \frac{1}{2s} + \frac{(1 - 2\rho_0)}{2(s + a - b)} + \left(\frac{1}{2s} - \frac{1}{2(s + a - b)} \right) \lambda_-^n \quad (66)$$

where $a = 2(1 + 2h)$, $b = 1 - 2\rho_0 + 1/(1 - 2\rho_0)$, and

$$\lambda_- = \frac{s + a - \sqrt{(s+a)^2 - 4}}{2}. \tag{67}$$

To obtain the explicit time dependence of the probabilities G_n, we invert equation (66) using the convolution theorem for the LT. We thus get

$$G_n(\tau) = \frac{1}{2} + \frac{n}{2} \int_0^\tau \frac{e^{-a\tau'} I_n(2\tau')}{\tau'} \, d\tau' + \left[\frac{(1 - 2\rho_0)^n}{2} - \frac{n}{2} \int_0^\tau \frac{e^{-b\tau'} I_n(2\tau')}{\tau'} \, d\tau' \right] e^{(b-a)\tau}. \tag{68}$$

In the limit $\rho_0 \to 1/2$, the difference equations for the $\hat{G}_n$ become homogeneous; the last term in (68) vanishes and one need compute only one remaining integral.

Determining the long-time asymptotics of the solution (68) requires separate analysis of two cases: $\rho_0 \leqslant 1/2$ and $\rho_0 > 1/2$. As we shall see, both cases yield the same expansion for $\rho(\tau)$.

For $n = 1$, the integrals in the right-hand side of (68) can be computed by making use of the identity [39]

$$\int_0^z \frac{e^{-\beta y} I_1(2y)}{y} \, dy = e^{-\beta z} \sum_{k=0}^\infty \frac{z^{2k+1}}{k!(2k+1)\Gamma(k+2)} {}_1F_1(1; 2(k+1); \beta z) \tag{69}$$

where ${}_1F_1(\alpha; \beta; \gamma)$ is a generalized hypergeometric function. For short times τ, however, it is easier to use the series expansion of the Bessel functions to evaluate the integrands. In this limit, we obtain, to second order:

$$\rho(\tau) = \rho_0 - 2(\rho_0^2 + h(2\rho_0 - 1))\tau - (2\rho_0^3 + \rho_0^2(1 + 8h) + 8h^2\rho_0 - 4h^2 - h)\tau^2 + \mathcal{O}(\tau^3). \tag{70}$$

The ascending series on the right-hand side of (69) is not suitable for the analysis of the long-time asymptotics. Instead, we observe that for $\rho_0 \leqslant \frac{1}{2}$ ($b \geqslant 2$), the integrals in (68) converge for $\tau \to \infty$. We can therefore split them into a definite and an indefinite part and use the adequate asymptotic expansion for the latter. This yields

$$\rho(\tau \to \infty) = \rho_s + (16\sqrt{\pi})^{-1} \left[\frac{1}{h} - \frac{1 - 2\rho_0}{\rho_0^2} \right] \tau^{-3/2} e^{-4h\tau} \qquad \rho_0 \leqslant \tfrac{1}{2}. \tag{71}$$

For $\rho_0 > \frac{1}{2}$ ($b < -2$), however, the last integral diverges. Nevertheless, we can split the integral as follows:

$$\int_0^\tau \frac{e^{-b\tau'} I_1(2\tau')}{\tau'} \, d\tau' = \int_0^{C_1} \frac{e^{-b\tau'} I_1(2\tau')}{\tau'} \, d\tau' + \int_{C_1}^\tau \frac{e^{-b\tau'} I_1(2\tau')}{\tau'} \, d\tau' \tag{72}$$

with a sufficiently large constant C_1, so that the second integral on the right-hand side can be well approximated by expanding the modified Bessel function to its leading term [35]. We can then replace the original integral by

$$\frac{1}{2\sqrt{\pi}} \int_{C_1}^\tau \frac{e^{(2-b)\tau'}}{\tau'^{3/2}} \approx C_2 - \frac{1}{\sqrt{\pi\tau}} e^{(2-b)\tau} + \sqrt{2-b} \, \text{erfi}\big(\sqrt{(2-b)\tau}\big) \tag{73}$$

where C_2 is a constant and the imaginary error function is defined as

$$\text{erfi}(x) = -i \, \text{erf}(ix) = \frac{2}{\sqrt{\pi}} \int_0^x e^{y^2} \, dy. \tag{74}$$

Thus, for $n = 1$, the last term in (68) becomes

$$-\frac{e^{(b-a)\tau}}{2} \int_0^\tau \frac{e^{-b\tau'} I_1(2\tau')}{\tau'} \, d\tau'$$

$$\approx -\sqrt{\frac{2-b}{\pi}} D\big(\sqrt{(2-b)\tau}\big) e^{(2-a)\tau} + \frac{1}{2\sqrt{\pi\tau}} e^{(2-a)\tau} + C_3 e^{(b-a)\tau} \tag{75}$$

where $C_3 = -C_2/2$ and $D(x) = \mathrm{e}^{-x^2} \int_0^x \mathrm{e}^{y^2}\, \mathrm{d}y$ is the so-called Dawson's integral [35]. For large arguments,

$$D(x) = \frac{1}{2x} + \frac{1}{4x^3} + \mathcal{O}\left(\frac{1}{x^5}\right). \tag{76}$$

If we now use (76) to expand the first term on the right-hand side of (75), we end up with

$$-\frac{\mathrm{e}^{(b-a)\tau}}{2} \int_0^\tau \frac{\mathrm{e}^{-b\tau'}\, I_1(2\tau')}{\tau'}\, \mathrm{d}\tau' \approx -\frac{1}{4(2-b)\tau^{3/2}}\, \mathrm{e}^{(2-a)\tau} + \mathcal{O}(\tau^{-5/2}\, \mathrm{e}^{(2-a)\tau}) + C_3\, \mathrm{e}^{(b-a)\tau}. \tag{77}$$

Clearly, the last, purely exponential term decays faster than all other terms, since $b < -2$. Thus, the leading order is the term proportional to $\tau^{-3/2}$. We then find the same decay law as for $\rho_0 < 1/2$, of equation (71). The relaxation time is universal and given by $\tau_R = 1/(4h)$.

The MF approximation is derived by noting that $G_1 = 1 - P_1$ and $G_2 = 1 - 2P_1 + 2P_2$ and using the factorization ansatz $P_2 = P_1^2$. This leads to

$$\frac{\mathrm{d}\rho}{\mathrm{d}\tau} = -2\rho^2 + 2h\,(1 - 2\rho). \tag{78}$$

The physical steady state of this equation is given by (63); this is not surprising, since the steady state is an equilibrium one, like in the reversible coalescence case. The early time behaviour is in agreement with equation (70) up to the first order, while the long-time approach of the MF solution to ρ_s is easily found to be

$$\rho^{\mathrm{MF}}(\tau) - \rho_s \propto 2\frac{(h^2+h)^{1/2}(\rho_0 - \rho_s)}{\rho_0 + (h^2+h)^{1/2} + h}\, \mathrm{e}^{-4(h^2+h)^{1/2}\tau} \qquad \tau \to \infty. \tag{79}$$

Once again, the MF approach fails to capture the time-dependent prefactor of the exponential in the exact solution, although it yields the correct relaxation time for large h.

In the small-h limit, the expressions for $\rho_s \approx h^{1/2}$ and τ_R agree with the continuum limit [26]. These results have also been obtained by Rácz by mapping the above model into the kinetic Ising model; to do so, one chooses $\Gamma = 2D/a^2$, $\delta = (1 - h)/(1 + h)$ and $w_i^{(2)}(\{\sigma\}) = 0$ in equation (59) [15]. This yields hopping to nearest sites at rate D/a^2, nearest-neighbour annihilation at rate $2D/(a^2(1 + h))$, and pair production at rate $2Dh/(a^2(1 + h))$, i.e. the dynamics of our model for small h. At larger h, however, the correspondence is lost because annihilation events in the spin model are slower than hopping onto empty sites. Our results are a natural generalization of Rácz's solution for the case of arbitrary h. In particular, in the large-h limit, the steady state coverage is given by equation (64).

We also find that the decay to the steady state is not purely exponential but rather given by a power of τ times an exponential. This corroborates a recent conjecture of Habib *et al* [27], based on the continuum approximation of equation (61).

Finally, we remark that the above model might capture essential features of transient optical absorption at energies less than the interband gap in certain one-dimensional organic semiconductors [40, 41]. It has been argued that the high-energy peak in the absorption spectrum of *trans*-polyacetylene may be due to the photogeneration of intrinsic, self-localized excitations of the semiconductor chain [41] in form of alternating soliton–antisoliton pairs which move randomly along the chain under the influence of thermal fluctuations and annihilate upon contact.

3.3. Annihilation with symmetric birth

The input process consists of a double-particle birth, i.e. a particle produces offspring at both neighbouring sites at rate V (on each side). In other words, we have the additional reactions

$SAS \rightarrow AAA$, $SAA \rightarrow AAS$, $AAS \rightarrow SAA$ and $AAA \rightarrow SAS$. The probabilities $G_n(t)$ obey the equations [26]:

$$\frac{dG_n}{dt} = (2D + 2V)(G_{n+1} - 2G_n + G_{n-1}) \qquad n > 1. \tag{80a}$$

The boundary condition is nontrivial; for $n = 1$, one has

$$\frac{dG_1}{dt} = 2D\,(G_2 - 2G_1 + 1) + 2V(G_2 - G_1). \tag{80b}$$

Notice that in the above equations we have set $a = 1$. This is done bearing in mind that there is no straightforward continuum approximation of the model, due to the form of the boundary condition. As before, we have the condition $0 \leqslant G_n \leqslant 1$. Again, we solve the set of equations (80) for an initially uncorrelated distribution given by the initial condition (57).

We study this model with and without diffusion. Let us first consider the case of $D = 0$. In this limit, clusters of particles can spread only by giving birth. To simplify the evolution equations for the G_n we let $\tau = 2Vt$ and $G_n(\tau) = \frac{1}{2}(1 + F_n(\tau))$. We then have the initial BVP:

$$\frac{dF_n}{d\tau} = F_{n+1} - 2F_n + F_{n-1} \tag{81a}$$

$$\frac{dF_1}{d\tau} = F_2 - F_1 \tag{81b}$$

$$F_n(0) = (1 - 2\rho_0)^n. \tag{81c}$$

The solution of these equations is readily obtained by LT methods similar to those used above. The LT of $F_1(t)$ takes the form

$$\hat{F}_1(s) = \frac{1 - 2\rho_0}{s - \upsilon} - \frac{\rho_0}{s - \upsilon}\left(\sqrt{\frac{s + 4}{s}} - 1\right) \tag{82}$$

where $\upsilon \equiv 4\rho_0^2/(1 - 2\rho_0)$. For three simple cases, $\rho_0 = 0$, $1/2$ and 1, the transform can be inverted to yield $G_1 = 1$, $1/2$, and $1/2\,(1 - e^{-2\tau}I_0(2\tau))$, respectively. These results merely indicate that an empty system remains empty; $\rho_0 = 1/2$ is the steady state coverage; and initially full lattices decay into the steady state.

We can also invert explicitly $\hat{F}_1(s)$ when $0 < \rho_0 < 1/2$. We get

$$F_1(\tau) = e^{\upsilon\tau}\left[1 - \rho_0 - \rho_0(\upsilon + 4)\int_0^\tau e^{-(\upsilon+2)\tau'}I_0(2\tau')\,d\tau'\right] - \rho_0 e^{-2\tau}I_0(2\tau). \tag{83}$$

Using the appropriate long-time expansion, we get

$$F_1(\tau) \approx \frac{1 - 2\rho_0}{\rho_0\sqrt{4\pi\tau}} \qquad \tau \rightarrow \infty \tag{84}$$

or, in terms of the coverage

$$\rho(\tau) = \frac{1}{2} - \frac{1}{2}F_1(\tau) \approx \frac{1}{2} - \frac{1 - 2\rho_0}{4\rho_0\sqrt{\pi\tau}} \qquad \tau \rightarrow \infty. \tag{85}$$

Thus the system decays algebraically into the steady state $\rho_s = 1/2$. In fact, Sudbury had shown that any homogeneous, random distribution leads to a half-empty lattice [26, 30]. It is therefore not surprising that we obtain the same behaviour also for $1/2 < \rho_0 < 1$. In this regime, $\upsilon < 0$, and the LT inversion becomes difficult. Since we are mainly interested in the long-time asymptotics of F_1, we circumvent this difficulty by expanding $\hat{F}_1(s)$ about $s = 0$ and making use of a Tauberian theorem. For $s \rightarrow 0$,

$$\hat{F}_1(s) \approx \frac{2\rho_0}{\upsilon \sqrt{s}} + \mathcal{O}(1) \tag{86}$$

implying that

$$F_1(\tau) \approx \frac{1 - 2\rho_0}{\rho_0 \sqrt{4\pi\tau}} \qquad \tau \to \infty. \tag{87}$$

This matches the result for $0 < \rho_0 < 1/2$.

We now turn to the case of annihilation with double birth and diffusion, $D > 0$. Again, we take equations (57) and (80) as a starting point; setting $\tau = 2(D+V)t$ and $G_n = \frac{1}{2}(F_n+1)$, and taking the LT with respect to τ, we finally obtain

$$\hat{F}_1(s) = \frac{1}{2}\left(\frac{\kappa}{s} - \frac{2\rho_0(1-\kappa)+\kappa}{s-\upsilon}\right)\left(\frac{\sqrt{s^2+4s}-s-2\kappa}{(1-\kappa)s-\kappa^2}\right) + \frac{1-2\rho_0}{s-\upsilon} \tag{88}$$

with $\kappa \equiv D/(D+V)$. Notice that we recover the appropriate solutions when $\kappa = 1$ and 0. These limits refer to the $V = 0$ and $D = 0$ cases, respectively. $\hat{F}_1(s)$ can be inverted for particular cases of the parameters ρ_0 and κ. However, it is simpler to make use of the $s = 0$ expansion to obtain the long-time asymptotics:

$$\hat{F}_1(s) \approx \frac{1}{s} - \frac{1}{\kappa\sqrt{s}} \qquad s \to 0. \tag{89}$$

This leads to

$$\rho \approx \frac{1}{2\kappa\sqrt{\pi\tau}} \qquad \tau \to \infty. \tag{90}$$

This result is not valid for $\kappa = 0$, since the limit $\kappa \to 0$ is singular. It is easy to see that the system cannot become empty without diffusion [30, 42]. In that case, (85) holds.

Let us compare the above results with the MF approximation, which can be derived from the equation for G_1 in the usual way. In the presence of diffusion, the simple MF approach yields

$$\frac{d\rho}{d\tau} = (1-\kappa)\rho - 2\rho^2. \tag{91}$$

Consequently, the steady states are $\rho_s = 0, (1-\kappa)/2$. Note that the existence of a non-empty steady state is already in contradiction with the exact solution (90). The nontrivial, time-dependent solution of (91) reads

$$\rho^{\mathrm{MF}} = \frac{(1-\kappa)\,\rho_0}{2\rho_0 + (1-\kappa-2\rho_0)\,e^{(\kappa-1)\tau}} \tag{92}$$

predicting exponential relaxation, in contrast to the inverse power law behaviour of the exact solution. Thus, for $\kappa > 0$, the MF approximation fails both at the static and the dynamic levels, whereas for $\kappa = 0$ (no diffusion), it describes the steady state correctly, but not the long-time dynamics. At the MF level, the effect of diffusion consists in driving the system from a steady state with half the lattice filled into a steady state with a smaller (but finite!) coverage. In contrast, the effect of diffusion on the exact solution is much more drastic, since the slightest amount of mobility already lands the system in an empty absorbing state. Note also the somewhat surprising fact that the presence of diffusion drives the steady state away from the MF prediction, except when the value of κ becomes close to one. In this limit, $\rho^{\mathrm{MF}}(\infty)$ again becomes arbitrarily close to zero.

4. Summary and outlook

We have derived a series of exact results for the one-dimensional kinetics of the lattice coverage and the particle concentration for coalescence and annihilation with various particle sources.

In the case of reversible coalescence the MF approach reproduces the equilibrium steady state correctly, but it only yields the relaxation time of the exact solution if h and ρ_0 are large enough. Besides, this approximation is not sensitive enough to reproduce the observed fluctuation-induced phase transition. In contrast, the off-lattice approximation valid for low input rates h (and thus for low transient concentrations) provides a good qualitative description of the long time asymptotics. For large h, no qualitative changes in the c_0 and τ dependence are observed, but the values of the prefactor and the relaxation time in the asymptotic form of the solution depend on the lattice constant a. For early times, we find that the exact solution is in agreement with the classical MF approach, while the off-lattice approximation dictates a slower kinetics in this regime (one expects a similar conclusion for the other lattice reactions studied in this paper).

In the case of coalescence and annihilation with single-particle input, the exact steady state is expressible in terms of Bessel functions. For small h-values, it is well reproduced by the continuum approach, whereas for large values, it becomes MF-like. In this case, the relaxation is purely exponential, and τ_R is again MF-like only for large h.

For annihilation with pair input, the steady state is an equilibrium state and can be derived directly from the MF approach. However, the relaxation is not purely exponential, as predicted by the MF approach, since the concentration behaves like $\tau^{-3/2}e^{-\tau/\tau_R}$ with a universal τ_R. In this case, the somewhat faster relaxation with respect to the single-particle case may be due to the higher particle input.

Summarizing, in the cases for which the continuum approximation was considered, the latter is in good qualitative agreement with the exact long-time kinetics and with the steady state in the low-h limit, however, deviations from the exact kinetics are expected for large values of h, i.e. at higher transient concentrations. In this limit, the MF approximation yields relatively good results for τ_R; even in the reversible coalescence case, provided that the initial concentration is sufficiently high. Fluctuations can also be safely neglected in the short-time regime.

As for annihilation with symmetric birth, we were able to confirm Sudbury's result for an infinite lattice, and prove that the long-time relaxation to the steady state is proportional to $\tau^{-1/2}$, both for immobile reactants and in the presence of diffusion. In the diffusionless case, the MF approach reproduces the exact steady state correctly, but not the long-time kinetics. Any amount of diffusion lands the system in an empty state, in contrast to the MF prediction.

Possible generalizations of our work include studying finite size effects and generalizing the method to better understand the spatial organization in these systems; in this respect, it is of interest to compute quantities such as interparticle distribution functions or multiple-point correlations from joint probabilities for pairs of intervals, both on-lattice and in the continuum limit [22]. The present methods also allow to study the effect of temporal correlations [20] or inhomogeneities in the initial conditions [24].

References

[1] Privman V (ed) 1996 *Nonequilibrium Statistical Mechanics in One Dimension* (Cambridge: Cambridge University Press)

[2] Schütz G M 2000 *Phase Transitions and Critical Phenomena* vol 19, ed C Domb and J Lebowitz (New York: Academic)

[3] Marro J and Dickman R 1999 *Nonequilibrium Phase Transitions in Lattice Models* (Cambridge: Cambridge University Press)

[4] Henkel M, Orlandini E and Santos J 1997 *Ann. Phys., NY* **259** 163

[5] Alcaraz F C, Droz M, Henkel M and Rittenberg V 1994 *Ann. Phys., NY* **230** 250

[6] Privman V, Cadilhe A M and Glasser M L 1995 *J. Stat. Phys.* **81** 881

[7] ben-Avraham D, Burschka M and Doering C 1990 *J. Stat. Phys.* **60** 695

[8] Burschka M, Doering C and ben-Avraham D 1989 *Phys. Rev. Lett.* **63** 700

[9] Doering C R and ben-Avraham D 1989 *Phys. Rev. Lett.* **62** 2563

[10] Krebs K, Pfannmüller M P, Wehefritz B and Hinrichsen H 1995 *J. Stat. Phys.* **78** 1429

[11] Simon H 1995 *J. Phys. A: Math. Gen.* **28** 6585

[12] Mobilia M and Bares P A 2001 *Preprint* cond-mat/0107427

[13] Torney D C and McConnell H M 1983 *J. Phys. Chem.* **87** 1941

[14] Lushnikov A A 1987 *Phys. Lett.* A **120** 135

[15] Rácz Z 1985 *Phys. Rev. Lett.* **55** 1707

[16] Spouge J L 1988 *Phys. Rev. Lett.* **60** 871

[17] Family F and Amar J G 1991 *J. Stat. Phys.* **65** 1235

[18] Redner S and Kang K 1985 *Phys. Rev.* A **32** 435

[19] Privman V 1994 *Phys. Rev.* E **50** 50

[20] Grynberg M D and Stinchcombe R B 1996 *Phys. Rev. Lett.* **76** 851

[21] Henkel M and Hinrichsen H 2001 *J. Phys. A: Math. Gen.* **34** 1561

[22] Lin J C, Doering C R and ben-Avraham D 1990 *Chem. Phys.* **146** 355

[23] Peschel I, Rittenberg V and Schultze U 1994 *Nucl. Phys.* B **430** 633

[24] Alimohammadi M, Khorrami M and Aghamohammadi A 2001 *Preprint* cond-mat/0105124

[25] Masser T and ben-Avraham D 2000 *Phys. Lett.* A **275** 382

[26] Masser T and ben-Avraham D 2001 *Phys. Rev.* E **63** 066108

[27] Habib S, Lindenberg K, Lythe G and Molina-Paris C 2001 *Preprint* cond-mat/0102270

[28] Abad E, Frisch H L and Nicolis G 2000 *J. Stat. Phys.* **99** 1397

[29] Rácz Z 1985 *Phys. Rev. Lett.* A **32** 1129

[30] Sudbury A 1990 *Ann. Prob.* **18** 581

[31] Lin J C 1992 *Phys. Rev.* A **45** 3892

[32] Carslaw H S and Jaeger J C 1959 *Conduction of Heat in Solids* 2nd edn (Oxford: Clarendon)

[33] Doetsch G 1943 *Theorie und Anwendung der Laplace Transformation* (New York: Dover)

[34] Feller W 1971 *An Introduction to Probability Theory and its Applications* vol 2, 2nd edn (New York: Wiley)

[35] Abramowitz M and Stegun I 1972 *Handbook of Mathematical Functions* (New York: Dover)

[36] Wall H S 1948 *Analytic Theory of Continued Fractions* (Princeton, NJ: Van Nostrand-Reinhold)

[37] Peliti A 1986 *J. Phys. A: Math. Gen.* **19** L365

[38] Friedlander K 1977 *Smoke, Dust and Haze: Fundamentals of Aerosol Behavior* (New York: Wiley)

[39] Luke Y L 1962 *Integrals of Bessel functions* (New York: McGraw-Hill)

[40] Su W P and Schrieffer J R 1980 *Proc. Natl Acad. Sci. USA* **77** 5626

[41] Orenstein J and Baker G L 1982 *Phys. Rev. Lett.* **49** 1043

[42] ben-Avraham D, Leyvraz F and Redner S 1994 *Phys. Rev.* E **50** 1843